PIVOTED-PAD JOURNAL GAS BEARING PERFORMANCE IN EXPLORATORY OPERATION OF BRAYTON CYCLE TURBOCOMPRESSOR

by Robert Y. Wong, Warner L. Stewart, and Harold E. Rohlik

Lewis Research Center
Cleveland, Ohio

TECHNICAL PAPER proposed for presentation at

Second International Symposium on Gas Lubrication Design Application and Exhibit sponsored by the Lubrication and Nuclear Divisions of the American Society of Mechanical Engineers and the Office of Naval Research ONR
Las Vegas, Nevada, June 10-17, 1968

NATIONAL AERONAUTICS AND SPACE ADMINISTRATION

PIVOTED-PAD JOURNAL GAS BEARING PERFORMANCE IN EXPLORATORY OPERATION OF BRAYTON CYCLE TURBOCOMPRESSOR

by Robert Y. Wong, Warner L. Stewart, and Harold E. Rohlik

Lewis Research Center
National Aeronautics and Space Administration
Cleveland, Ohio

E-4237

ABSTRACT

This paper describes findings obtained to date in the area of journal gas bearings from an experimental study of a Brayton Cycle turbocompressor designed for the requirements of a two-shaft - 10-kilowatt space power system. The journal bearing design utilizes three pads pivoted on conforming balls and sockets. Two of the pivots are rigidly mounted to the frame, and the third pivot is mounted to the frame through a low-spring-rate diaphragm.

The paper describes the salient package and bearing design features and then presents the principal results obtained from testing the package in both a spin calibration rig and operation at design temperature conditions with an inert gas. The results discussed include (a) the successful use of a pneumatic loading device to vary pad load during operation, (b) the operating characteristics of the bearings as obtained over a range of pad loads and ambient conditions, (c) structural and dynamic behavior of the bearing-support system during design temperature operation, and (d) a discussion of the wear characteristics of the conforming ball and socket pivot as obtained from the tests made to date.

TM X-52372

INTRODUCTION

The NASA Lewis Research Center is currently conducting a technology program involving the study of the closed-loop Brayton Cycle power system for space auxiliary electric power. This system uses a gas turbine engine to convert heat energy to electric power, and it includes the necessary compressor, turbines, and generator for power conversion as well as appropriate exchangers for heat input and rejection. An inert gas was selected as the system working fluid because of its obvious advantage from the standpoint of materials corrosion. In such a space power system, it is desirable to utilize gas bearings in the rotating machinery. The use of this type bearing, as opposed to rolling element bearings, eliminates the need for an oil lubrication and associated sealing systems. Also, this would reduce bearing power loss and offer a potential for achieving the long life desired for these systems. Gas bearings have been successfully used in certain ground applications, which tends to substantiate the potential ascribed to this bearing system (ref. 1).

To explore problems associated with the application of gas bearings to a space power system, a program that has been under way at the NASA Lewis Research Center involves power packages designed for representative Brayton space power applications. One such package is a turbocompressor unit designed as part of a two-shaft power system (see ref. 2 for a description of the reference system). This package includes a centrifugal compressor and a radial inflow turbine on a common shaft that is rotating on self-acting or hydrodynamic journal and thrust bearings. Reference 3 presents a detailed description of this package design.

Experimental performance of the turbocompressor as related to the journal bearings is presented herein. The salient features of these bearings include three pads pivoting on conforming balls and sockets with the capability for both self-acting and externally pressurized operation. Compensation for thermal growth is accomplished by mounting one of the pivots on a flexible diaphragm. The other two pivots are mounted rigidly to the frame.

Included in this paper is a description of the package and journal bearings, as well as the instrumentation used to determine the pad load and dynamic behavior of the bearing. Results obtained from the variation of pad load at high speed with a pneumatic load device are also described along with the calibrations of the bearing system and the film stiffness. The successful use of a pneumatic-diaphragm load device for pad load adjustments during hot package operation, and results obtained to date regarding observed wear characteristics of the conforming ball and socket pivots used in this package will also be discussed.

TURBOCOMPRESSOR DESCRIPTION

The turbocompressor has a centrifugal compressor driven at 38500 rpm by a radial-inflow turbine. Gas temperatures range from 1500°F at the turbine inlet to 76°F at the compressor inlet. Figure 1 shows the relative sizes of the various components and the arrangement of parts. The compressor and turbine rotors have tip diameters of 6 inches, the journal diameter is 1.75 inches, and the thrust-runner diameter is 3.24 inches. The total rotor weight is 19 pounds, and the overall rotor length is 19 inches. Detailed design information on this machine is presented in reference 3.

Each journal bearing includes three pivoted pads, as shown in the cross section in figure 2 The pivot of each pad is located 65 percent of the pad length from the leading edge One pad is mounted on a low-spring-rate (2000 to 4000 lb/in.) diaphragm that is deflected during assembly to preload the bearing. This diaphragm is used to accommodate limited amounts of thermal distortion, thus maintaining bearing preload in the zero-gravity space environment and in the vertical shaft position during ground testing. The shaft is clamped in place by this applied preload until external pressurizing gas is supplied through a central hole in each pivot to four orifices in the bore of each pad. A cross section of the flex-mounted journal bearing pad is shown in figure 3. Each pivot consists of a 0.5-inch-diameter tungsten carbide ball sliding in a conforming socket of A286 iron base alloy with a tungsten carbide coating. The conforming ball and socket was used to provide a gas seal in the pivot and to make the bearing self-aligning. The bore of the pads and the shaft journal were coated with tungsten carbide to provide some tolerance to light contacts between the two. Estimated friction power loss totals 120 watts for the six pads. The bearing load may be changed remotely by means of pressure in a closed cavity acting on one side of the flexible diaphragm (see figure 3).

The thrust bearing consists of a smooth runner coated with tungsten carbide and uncoated stator surfaces on either side of the runner. One of the stators employs the Rayleigh step design with eight lands to support the thrust load during normal operation. The other stator is a plain surface. Both are equipped with orifices for external pressurization during start and shut down; four in alternate lands of the stepped stator and six equally spaced around the smooth stator.

The thrust runner runs between the two stator surfaces with a total axial clearance of 0.005 inch. The total estimated power loss is 120 watts total for both the loaded stepped face and unloaded smooth face.

Figure 1 also shows design features employed to minimize temperatures and temperature gradients in the bearing areas. These features include thermal barriers near the hot turbine in the form of reflective heat shields and thin-wall sections in the shaft and in the struts of the main frame. Copper inserts in the struts and the shaft transmit bearing power losses and heat from the turbine to the compressor, which serves as a heat sink. A small quantity of cooling gas flows over the journal bearing pads and through the labyrinth seals into the turbine and the compressor.

BEARING SYSTEM INSTRUMENTATION

Experimental evaluation of the turbocompressor bearings required knowledge in three major areas: shaft and bearing component motions, bearing load, and the bearing environmental pressures and temperatures. Shaft motions relative to the frame were determined with two noncontacting-capacitance-sensitive displacement probes located 90° apart in radial planes near each journal bearing (fig. 2). Two probes of the same type were mounted on opposite sides of the thrust bearing to measure film thickness and relative motion between the thrust bearing runner and the stator. Two displacement probes were used to monitor the radial motions of the flex-mounted pivots of the turbine and compressor journal bearings (fig. 3). In addition, two displacement probes were used to monitor the radial motion of the leading edge of one of the fixed mounted pads of the turbine journal bearing to indicate pitch and roll motion of this pad.

The initial assembly of the turbocompressor included straingages mounted on the journal-bearing diaphragm to measure strain and, consequently, bearing load. Thermal sensitivity of the straingages led to alternate load-measuring methods, which included the displacement probe mounted on the bearing carrier (as shown in fig. 3) to sense pivot radial motions and diaphragm deflection. The diaphragm spring rate together with measured diaphragm deflection gives the bearing load. A second method used to indicate the load was based on the relation between self-acting film pressure and pad load. This relation was determined experimentally by externally pressurizing the closed volume on the back side of the diaphragm to change pad loading during operation.

Fifty-four thermocouples were used to measure the internal temperatures of the turbocompressor. These were in selected locations on bearing parts, the radiation shields, and structural members. Temperature measurements were examined for confirmation of calculated temperature distributions and thermal growth of parts. Similarly, pressure sensors and flowmeters were used to measure bearing cavity pressure, external bearing supply pressures, self-acting pressure in the journal bearing film, coolant pressures and flow rates, and diaphragm load pressure. Shaft speed was measured using a magnetic pickup and siz magnetic blocks imbedded in the shaft.

The most important measurements were displayed during operation, and all data were recorded on magnetic tape for analysis subsequent to package operation. Details on the instrumentation are included in reference 4.

CALIBRATION TECHNIQUES

The maintenance of pad load within narrow limits in gas journal bearings is essential to satisfactory operation. If the pad load becomes excessive, the gas film becomes dangerously thin and friction power loss becomes excessive. On the other hand, if the pad load becomes too low, the operation of the rotor-bearing system becomes unstable. In either case, bearing failure is likely to occur.

In the subject turbocompressor, the turbine and compressor are outboard of the gas-bearing support system (see fig. 1). Heat flow from the turbine toward the compressor and frictional power consumption in the bearings can cause thermal gradients, which may bring about differential growths. These, in turn, can have large effects on pad load and the subsequent operation of the gas bearing. It is therefore evident that, until these machines are fully qualified, continuous monitoring of the pad load is required, particularly during transient operation.

In the subject turbocompressor package, the pad load could be determined by measuring diaphragm deflection and applying a known diaphragm spring rate. Diaphragm spring rates may be easily determined for cold or hot isothermal conditions prior to assembly. In the package, however, the diaphragms are subjected to distortion when they are assembled to the bearing carrier and when they are subjected to nonisothermal conditions. These distortions can have unpredictable effects on the diaphragm spring rate. The change in spring rate resulting from distortion during assembly may be obtained by calibration after assembly. The change in spring rate due to thermal gradients, however, results in a degree of uncertainty with regard to the pad load as determined by this method at hot operating conditions.

In view of this uncertainty, a method for pad loaded determination based on the relation between hydrodynamic pressure generated between the pad and shaft and the pad load, was developed. This relation was determined experimentally, and the independent variables were assumed to be bearing ambient pressure, temperature, and speed. The bearing was operated at ambient pressures of 20 and 12 psia over a range of speeds from 30000 to 38500 rpm. The pad load was varied from 7 to 19 pounds by use of the pneumatic-load device described in the section Turbocompressor Description. The temperatures of the turbine and compressor journal bearings were 250° and 300°F, respectively. The effects of gas-viscosity change from these temperatures to the 500°F-operating temperature are negligible. Analysis of data showed that the pressure difference between the ambient pressure and the average hydrodynamic film pressure at the 12 orifices of each bearing was largely a function of the pad load. The data obtained for 12- and 20-psia ambient pressures and rotor speeds are presented in figure 4. From the figure, it can be seen that the gas pressure rise measured in the self-acting film is directly proportional to the pad load.

Data taken during the preceding calibration were also used to calculate bearing system stiffness for an external force applied radially to the pad through the pivot. Figure 5 presents a schematic of the bearing system. In the preceding calibration, the pneumatic load ΔF was applied radially to the pad through the pivot, as shown in figure 3. The deflection ΔX of the pivot (or pad) was measured. The spring rate of the diaphragm-pad-film system was obtained as the ratio of applied load to measured deflection $K_P = \frac{\Delta F}{\Delta X}$ and is plotted in figure 6 as a function of pad load for operation

under external pressurization and also under self-acting operation with ambient pressures of 20 and 12 psia.

From figure 6, it can be seen that, at 30000 rpm for externally pressurized operation, the system spring rate varies from 6000 to 20000 pounds per inch from a range of pad load from 8 to 22 pounds. For self-acting operation at an ambient pressure of 20 psia, the system spring rate varied from 6000 to 56000 pounds per inch for a range of pad load from 6.8 to 18 pounds. For self-acting operation at an ambient pressure of 12 psia, the system spring rate varies from 7000 to 90000 pounds per inch for a pad load range from 9 to 16 pounds. Thus, for a given pad load, self-acting operation gives a higher spring rate than that given for externally pressurized operation. It is further seen that the lower the bearing ambient pressure is at a given pad load, the higher the system spring rate of the bearing. This is the result of the thinner gas film that is associated with lower ambient pressure operation. In the range near 8 pounds of pad load, the bearing spring rate approaches the same value regardless of the type of operation.

Film spring rate was calculated from

$$K_f = 3\ (K_P - K_D)$$

where

K_f gas film spring rate

K_P system rate for external force on pad

K_D diaphragm spring rate

This equation assumes that film spring rates under all three pads are equal. Plotted in figure 7 is the film spring rate computed for self-acting operation

at ambient pressures of 20 and 12 psia and for externally pressurized operation of an ambient pressure of 20 psia. As can be expected, the bearing-film spring rate displays trends similar to those of the system spring rate. In the region of a 4-pound pad load, where unstable operation was initially observed, the gas-film spring rate was extrapolated to be 4000 to 5000 pounds per inch.

From these gas-film spring rates, the bearing-system spring rate K_S for an external force applied to the shaft in the direction of the diaphragm-mounted pad, was obtained from

$$K_S = \frac{K_f K_D}{K_D + K_f} + \frac{K_f}{2}$$

The system spring rate K_S is plotted as a function of pad load in figure 8 for self-acting operation with ambient pressures of 20 and 12 psia, and for externally pressurized operation at an ambient pressure of 20 psia. From these curves, if the pad load is known, the system spring rate may be obtained and the first and second natural frequencies can be computed. The frequencies so calculated will be approximate because K_S at the critical speeds may not be the same as that at the higher operating speed. For the subject turbocompressor, the pad loads in the turbine and compressor bearings at startup are 19 and 21.5 pounds, respectively. The turbine and compressor bearing spring rates corresponding to these loads are 20000 and 28000 pounds per inch, respectively. The first and second natural frequencies for the subject turbocompressor were computed to be 6500 and 10000 rpm without considering frame stiffness or package support stiffness.

In addition to these calibrations, reference values of unbalance, diaphragm motions, and leading edge motion of one pad of the turbine journal bearing were obtained. The mass eccentricity was 0.00017 inch at the turbine end, and 0.00012 inch at the compressor end. The radial motion of the pivot of the flex-mounted pad was about 1.5 times the motion of the shaft at all speeds above the natural frequencies for this machine. The leading edge motion of one of the fixed mounted pads in the turbine journal bearings varied between 0.00012 and 0.00028 inch depending on load, speed, and ambient pressure.

HOT OPERATION

Pad load as a function of time is plotted in figure 9 for a typical test of the subject turbocompressor at design temperature. Time zero is taken at the point when an injection start was made. At time minus 2/3 hour, just before the external pressurization is applied, the pad load shown is due to the clamping force exerted by the diaphragm of the flex-mounted pad. After the application of external pressurization, there is an 8- to 9-pound increase in pad load. After injection, the pad load increases about 2 pounds as the package is accelerated to about 95 percent speed. This increase in load is due to centrifugal and thermal effects from friction in the bearings. Then as heat from the turbine is conducted into the package, the pad load decreases as shown until at 3 hours after injection, thermal equilibrium is approached and the pad load levels off. In making the transition to self-acting operation, the external pressurization is shut off, and there is a loss in pad load of approximately 6 pounds.

At the end of the transition to self-acting operation, the turbine journal bearing load was down to 8.2 pounds, and the compressor journal bearing pad load was down to 12.2 pounds. It was observed that the turbine journal bearing was operating unstably while the compressor journal bearing appeared to be operating normally. This instability appeared as an unsteadiness in the position and shape of the orbit. It can be seen that the turbine journal pad load continued to drop off slightly between 3 and 6 hours. The continued loss in pad load was accompanied by an increase in the amplitude of the instability. A photograph of the shaft orbit pattern for the compressor and turbine journal bearings as obtained with proximity probes is presented in figure 10. It can be seen from the turbine journal orbit that the shaft is moving erratically in what appears to be a figure eight. It can also be seen that the compressor journal orbit is normal except for small disturbances in the orbit that seem to be transmitted from the turbine journal bearing. Figure 11 shows a shorter exposure of the instability in the turbine journal bearing. The inside loops that are characteristic of fractional frequency whirl can clearly be seen. Inspection of the probe traces of shaft motion on a time scale showed that the instability was a 1/6-fractional frequency whirl, about the same frequency as the first natural frequency. The whirl in the turbine journal bearing was suppressed by the application of 3.5 pounds of pneumatic load. The pneumatic load resulted in an increase of about 2 pounds in turbine pad load, as shown in figure 9. A photograph of the orbits after the increase in pad load of 2 pounds in the turbine journal shows that the orbits have returned to normal (fig. 12).

With reference to figure 9, it can be seen that after the initial application of the 3.5-pound pneumatic load, the pad load dropped only slightly in the next 2 hours of testing. At about 9 hours, in preparation to reduce the bearing ambient pressure, the pneumatic load was increased from 3.5 to 6 pounds. This increase was made as a precautionary measure because reduction in bearing ambient pressure reduces the pad load and cooling flow rate. A reduction in cooling flow rate will cause the bearing to operate at a higher temperature, which could lead to a lower pad load. The test was completed at $13\frac{1}{3}$ hours with no further observation of unstable operation.

Further analysis of data taken during the test showed that, although the orbit returned to normal after the application of the pneumatic load, the leading edge of the pad that was monitored during the test showed an irreversible increase in the amplitude of motion. The pitching motion of the pad had increased with no increase in unbalance.

A subsequent test further showed that whirl began at a higher value of pad load. In a similar manner to the previous test, the whirl was suppressed and even though the orbit returned to normal, there was a further increase in the amplitude of pitching motion of the pad. The amplitude of the pitching motion had gradually increased to a value ten times that observed in initial calibration tests. It was further observed that, at high values of pad load, the amplitude of pad pitching would increase and a synchronous roll motion would be superimposed. Then, as the pad load was decreased, the pitching motion would decrease and the roll motion would fade out. At one point in this test, the pad went into a slow roll for about 4 shaft revolutions, and

then the leading edge motions suddenly became violently erratic, which caused contacts leading to failure and the shaft deceleration from 36700 rpm to a stop in 1.7 seconds.

The tests described herein showed that, with the use of the pneumatic load device, pad load was controlled so that stable motion of the rotor could be maintained and the test could be continued. Also, an increased pad load was necessary to suppress a 1/6-fractional frequency whirl, and a gradual increase in the amplitude of pad pitch occurred, which suggests that there was a gradual change in the character of the pivots.

CONFORMING PIVOT WEAR INDICATIONS

As indicated in the description of the journal bearing design, conforming ball and socket pivots were used. These pivots provided the necessary freedom of pad motion and a means for introducing jacking gas without excessive leakage. In review, the ball was 1/2 inch in diameter and was fabricated from tungsten carbide. The associated socket, on the other hand, was formed as part of the A286 iron-base alloy shoe onto which a tungsten carbide coating was applied to the socket surface by use of a flamespraying technique. Lapping of the ball and socket surfaces was then performed to obtain the desired conformity. This design was intended (a) to provide the required seal for the external pressurization and for the hydrodynamic gas film without an additional complication such as O-rings, and (b) to give low contact stresses to enhance the life aspects of the pivot.

This conforming pivot design, however, has some questionable aspects regarding its performance and life that may negate the advantages just cited. First, because of the conforming fit, sliding motion will occur as the shoe

moves in response to shaft motions and hydrodynamic gas forces. The amplitude of such pivot sliding would be increased in proportion to the unbalance of the rotating assembly. This movement could result in fretting in the contact areas, which can occur even though the stress level is low. Second, the sliding friction can have an effect on the dynamics of the shoes, since a substantial moment arm (1/4 in) exists. Finally, another area of concern is the inability of any debris, if formed due to fretting between the ball and socket, to move out of the contact area. As a result, particles trapped between the surfaces in relative motion would create additional wear debris through a plowing and galling action. Such a problem was of particular concern in the subject design since the socket was flamesprayed, and a bond failure could result in additional debris.

During the course of the hot package tests, the problems just described appeared to manifest themselves over a rather short period of operating time. Contributing to this was that the balance of the rotor was not as precise as desired for a gas bearing machine (mass eccentricities at the compressor and turbine shaft ends were approximately 0.00012 and 0.00017 inch, respectively). This unbalance and associated eccentricity resulted in motion of the shoes, particularly in the pitching mode (as observed from proximity probe traces). Then during the hot testing, the amplitude of the pad pitch tended to increase with time, together with a requirement of increased pad loading to suppress unstable rotor operation. Thus, it appeared that with time, there was a change in the character of the pivot operation that could result from damage to the pivot surfaces.

During the last run made as of this writing, the pad pitching motions were quite large, with stable operation maintained only with rather large pad

loading. These observations were made during externally pressurized operation, and when self-acting operation of the turbine bearing was attempted, the seizure that was mentioned previously occurred, terminating the test. An examination of the proximity probe traces describing the various shaft and shoe motions during the seizure indicated that initial indication of "abnormal" motion was from the leading edge probes on the turbine bearing shoe. Extensive examination of all the motions was subsequently made, but no firm conclusions were drawn with regard to the dynamics of the bearing as contributing to the seizure.

Examination of the pivots, however, tended to substantiate the observations of the preceding tests that the pivot was changing in character, even to a point where seizure might be attributable to this cause. The examination indicated changes in the pivot surface characteristics, with particular degradation of the turbine bearing pivots. For example, presented in figures 13(a) to (d) are photos of the ball and socket associated with the flexible mount for both the turbine and compressor bearing. From this figure, little evidence of damage can be seen for the compressor bearing pivots, while substantial change in surface character is seen for that at the turbine end. In addition to the general degradation of these surfaces, patterns of the type expected due to the fretting action of particles between conforming surfaces can be seen (the I- and Z- patterns). This observation tends to substantiate the concern regarding the ability of the fully conforming pivot to accommodate debris formed during operation.

Even though substantial damage could not be observed visually for the compressor bearing pivots, initial phases of wear and damage became evident upon microscopic examination. This indicated that, although degradation of

the pivots at this end had not progressed to the extent of that at the turbine end, such damage was in the incipient stage.

It was considered of interest to examine the ball and socket contours in the heavily damaged regions to establish the changed surface character. Figure 14 presents typical trace results for the ball and socket of one of the turbine pivots. Inspection of the figure indicates that material was removed from the socket and attached to the ball, forming peaks and valleys as high as 0.0005 inch. From these traces, it is evident that the changes in surface character must have drastically changed the friction and pivoting behavior of the pivots.

From this examination, it is evident that the specific pivot configuration used in the turbocompressor package is deficient. However, a general conclusion regarding the inadequacy of the conforming pivot for this design cannot at present be made because of the possibility that the failure resulted from a bond failure of the coating in the socket. Thus, the elimination of the flamesprayed coating in the socket and the substitution with solid inserts may provide a satisfactory solution. Another possibility is to use some technique to permit debris to quickly leave the contact area and thus permit satisfactory performance for a reasonable length of time. On the other hand, the sliding movements of this design might be incompatible with the long-term operational life required of space power applications. Therefore, a continuing effort is being expended toward further defining the capability of this type pivot as well as examining alternate concepts (such as the nonconforming pivot) for this application.

CONCLUDING REMARKS

Presented herein was a description of pertinent results obtained to date in the investigation of the three-pad gas journal bearing configuration utilized in a Brayton turbocompressor package. From both cold-spin tests and hot-loop operation, it was indicated that, given proper environmental conditions, the bearing configuration was aerodynamically satisfactory under both externally pressurized and self-acting operating conditions. The low-spring-rate flexible diaphragm used for loading was also satisfactory for small differential thermal growths. In addition, the pneumatic loading device, incorporated into the unit as a modification, provided an excellent calibration tool for varying the pad load during operation for the study of bearing system and film stiffnesses.

Problem areas indicated in the journal bearing and support design included a severe unloading tendency during hot operation as a result of thermal growth of the carrier. This growth reduced the diaphragm deflection and, hence, the pad load. Modifications to reduce this problem included changes in the design of the rigidly mounted pivots to produce a thermal compensation for the growth of the parts at temperature. In addition, there are indications that the conforming pivots used in this design might be unsuitable from a wear standpoint. Additional effort, however, is still required before conclusive results regarding this aspect can be obtained.

SYMBOLS

K_D Diaphragm spring rate

K_f Spring rate of gas film

K_P System spring rate for an external load applied to pad

K_S System spring rate for an external load applied to shaft

ΔF External force applied to pad

ΔX Deflection of pad under applied force

ΔY Deflection of shaft

ΔZ Deflection of gas film

REFERENCES

1. P. W. Curwen, "Operational Experience With Gas Bearing Turbomachinery", ASME Winter Meeting, New York, November 1966.

2. D. T. Bernatowicz, "NASA Solar Brayton Cycle Studies", presented at the Symposium on Solar Dynamics Systems, Solar and Mechanics Working Groups, Interagency Advanced Power Group, Washington, D. C., Sept. 24-25, 1963.

3. Anon., "Design and Fabrication of a High-Performance Brayton Cycle Radial-Flow Gas Generator", AiResearch Mfg. Co., Rep. No. APS-5200-R (NASA CR-706), February 1967.

4. R. Y. Wong, R. C. Evans, and D. J. Spackman, "Preliminary Experimental Evaluation of a Brayton Cycle Turbo-Compressor Operating on Gas Bearings", NASA TM X-52261, 1966.

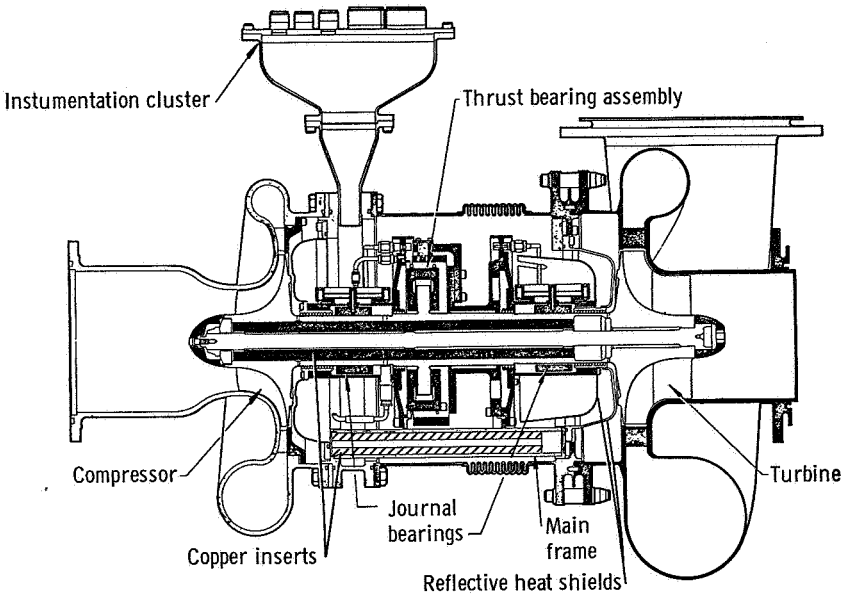

Figure 1. - Brayton-cycle turbocompressor.

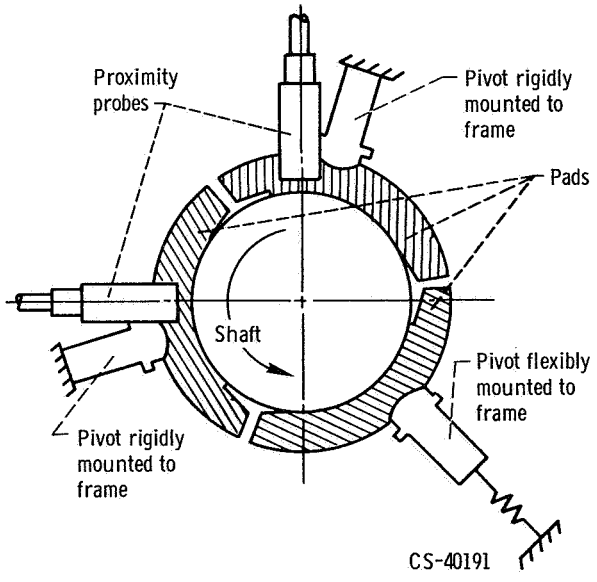

Figure 2. - Journal bearing cross section.

E-4237

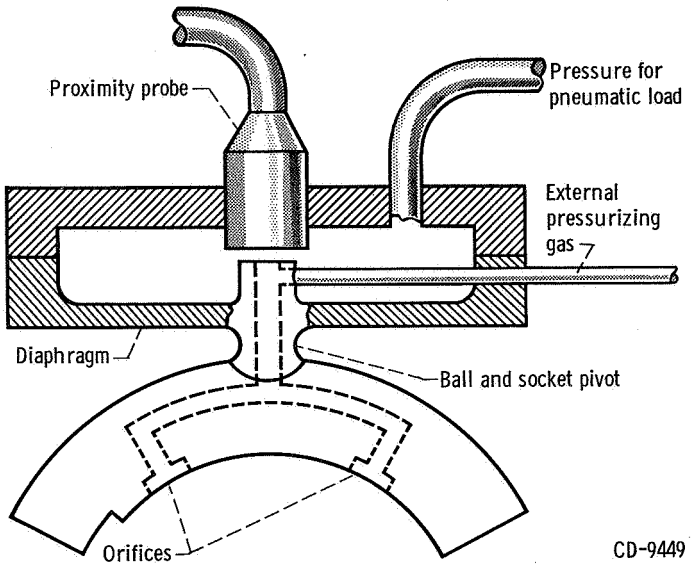

Figure 3. - Flexibly mounted pivot and pad with external pressurization arrangement, pneumatic load device and proximity probe.

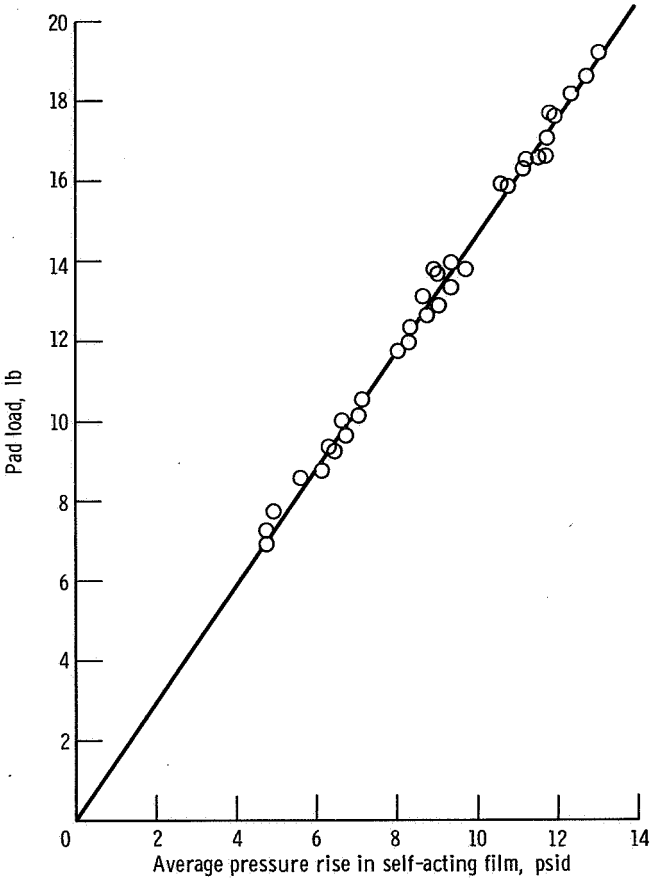

Figure 4. - Variation of pad load with pressure generated in self-acting film.

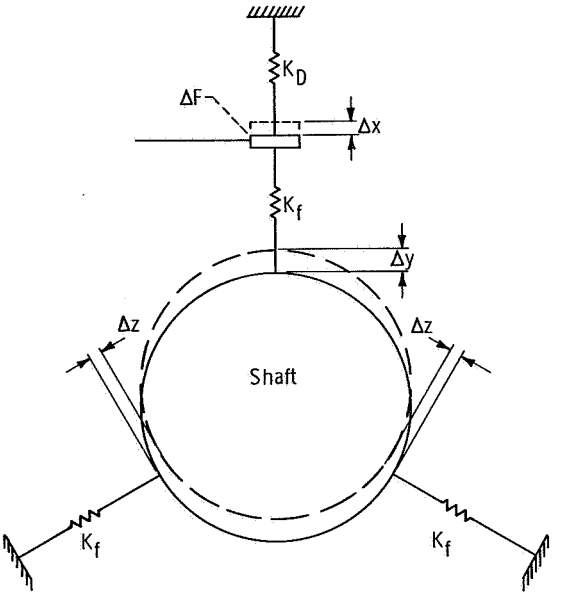

$K_p = \frac{\Delta F}{\Delta x}$ System spring rate for an external load applied to pad
K_D = Diaphragm spring rate
K_f = Spring rate of gas film
ΔF = External force applied to pad
Δx = Deflection of pad under applied force, ΔF
Δy = Deflection of shaft
Δz = Deflection of gas film

Figure 5. - Schematic of gas bearing.

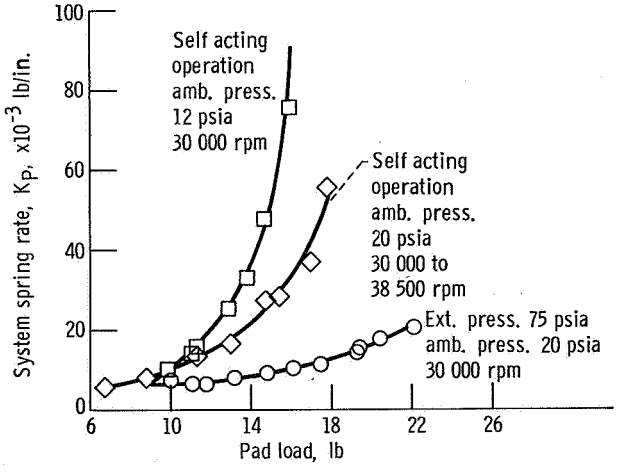

Figure 6. - System spring rate for an external force applied to pivot of pad.

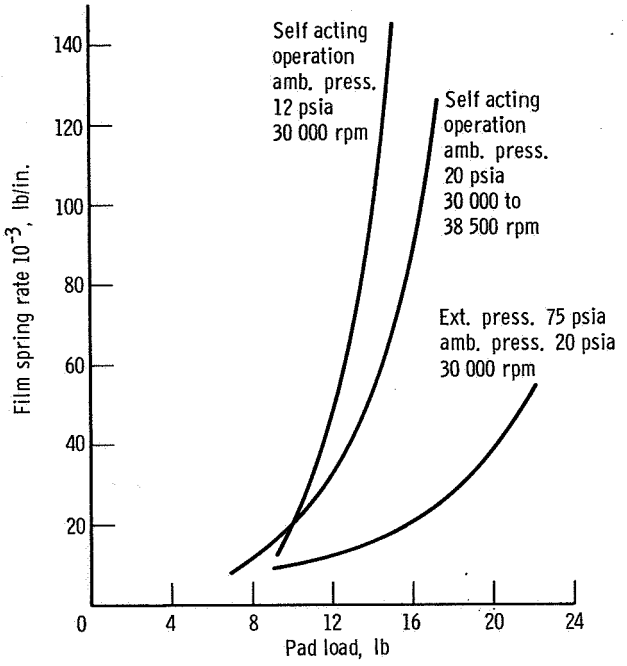

Figure 7. - Variation of gas film spring rate with pad load.

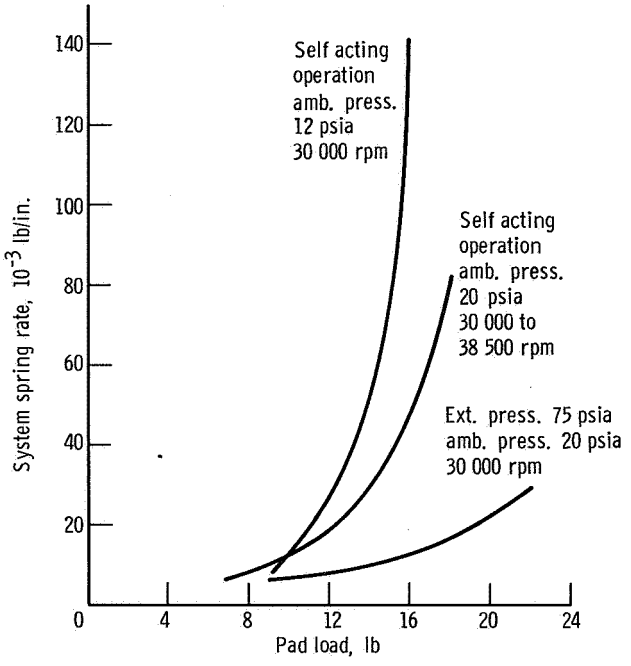

Figure 8. - Variation in system spring rate for external load applied to shaft.

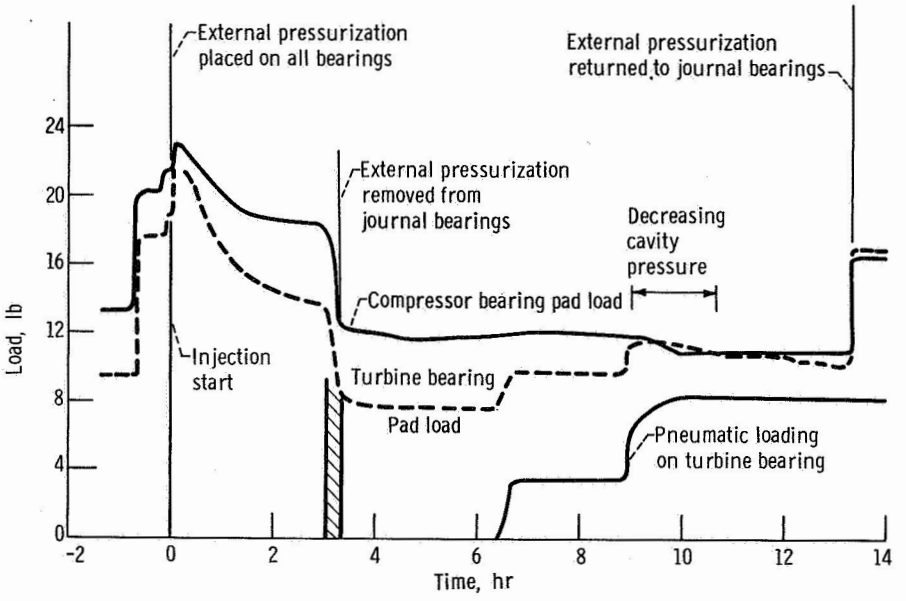

Figure 9. - Variation of pad load and pneumatic loading with time for a typical test.

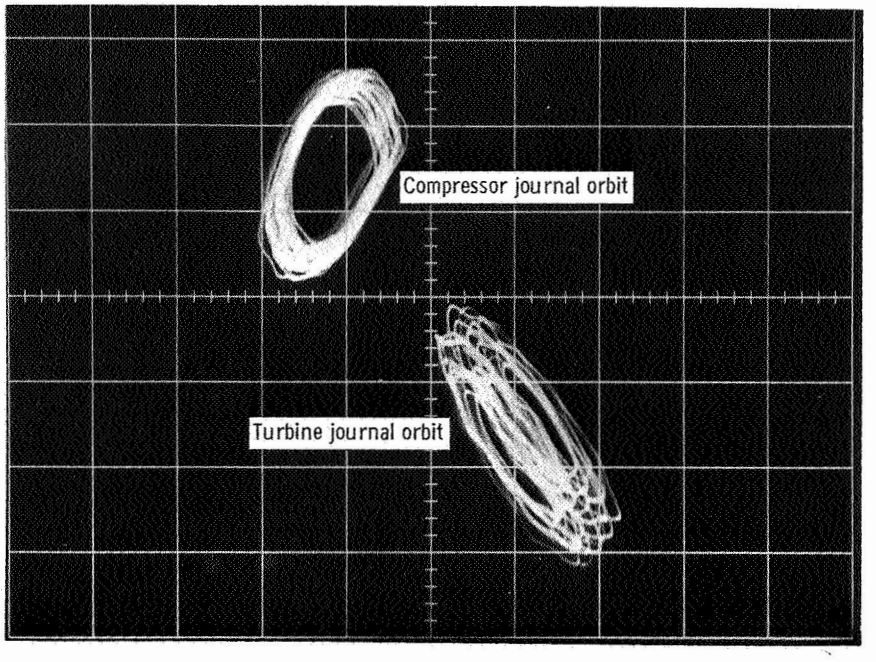

Figure 10. - Photograph of compressor and turbine journal bearing shaft orbits.

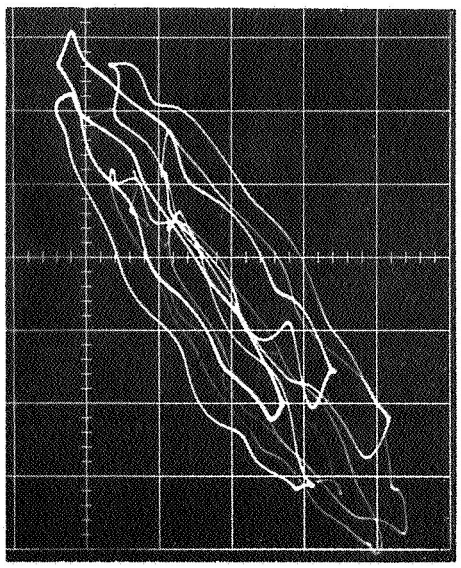

Figure 11. - Photograph of turbine journal bearing shaft orbit showing inside loops.

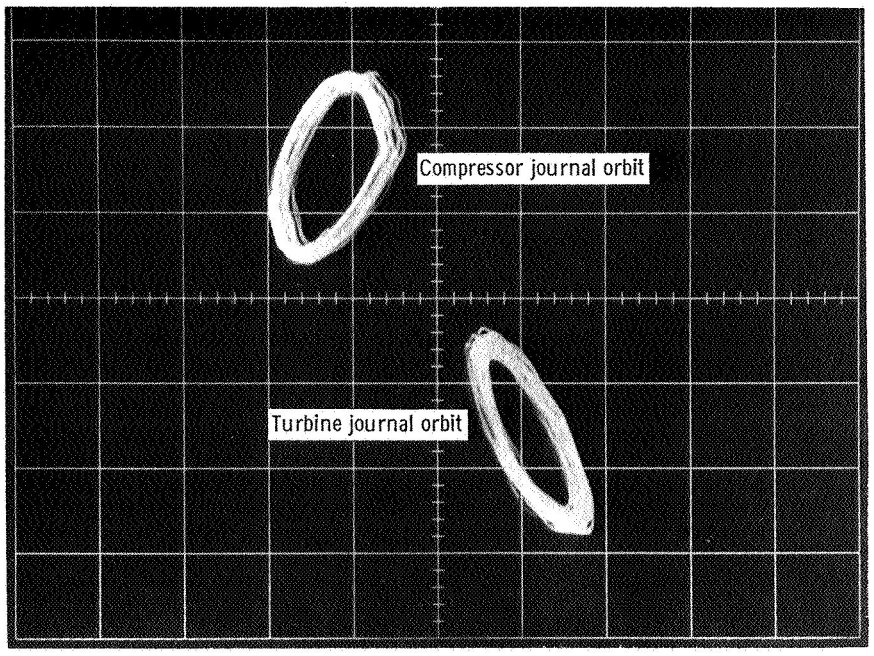

Figure 12. - Photograph of compressor and turbine bearing shaft orbits after the application of 3.5 pounds of pneumatic load on turbine bearing.

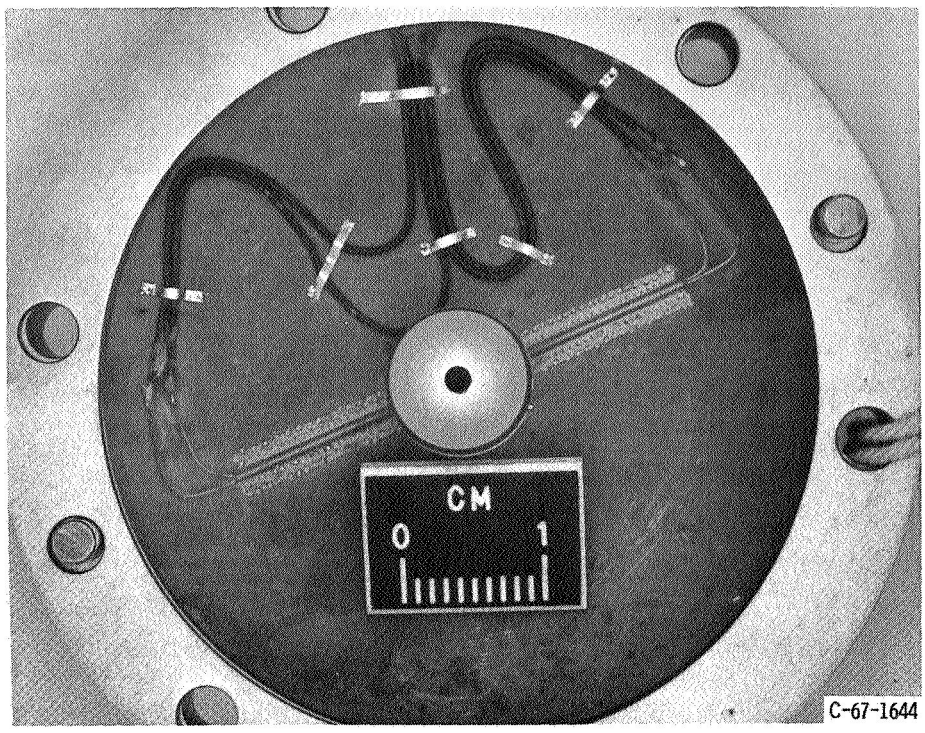

Figure 13 (a). - Ball of flex mounted pivot of the compressor journal bearing.

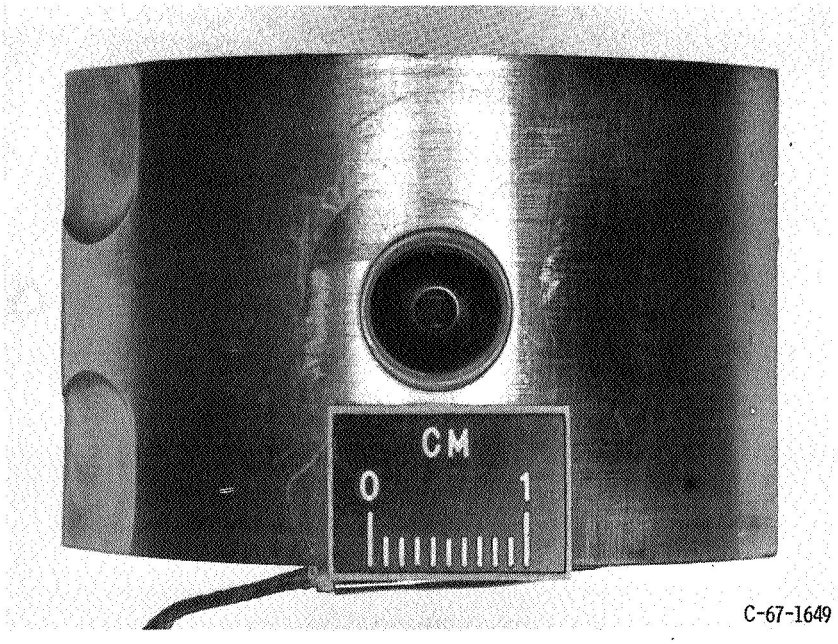

Figure 13 (b). - Socket of flex mounted pivot of the compressor journal bearing.

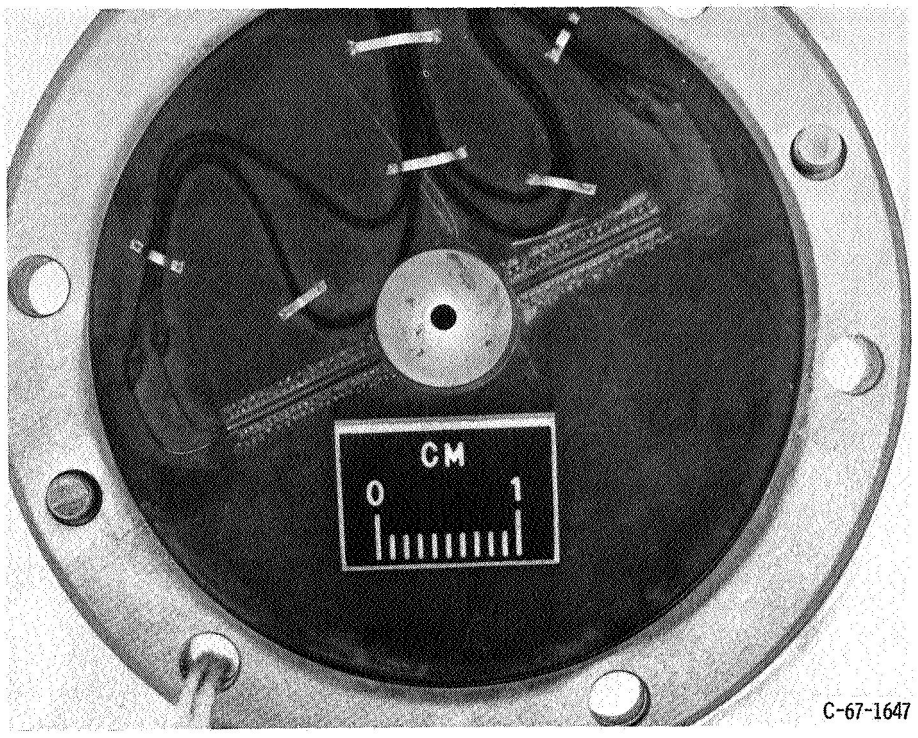

Figure 13 (c). - Ball of flex mounted pivot of the turbine journal bearing.

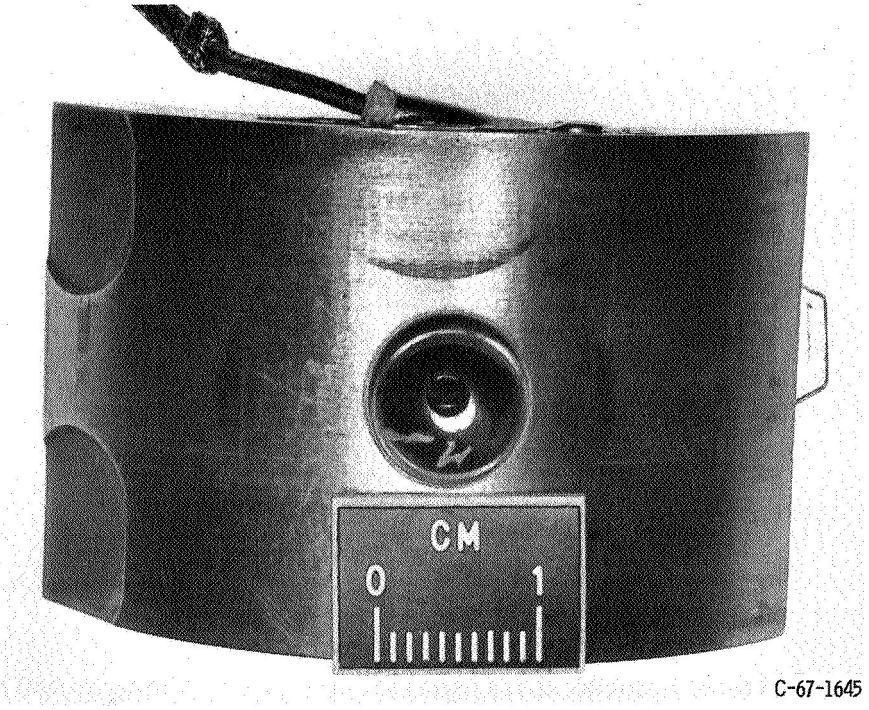

Figure 13 (d). - Socket of flex mounted pivot of the turbine journal bearing.

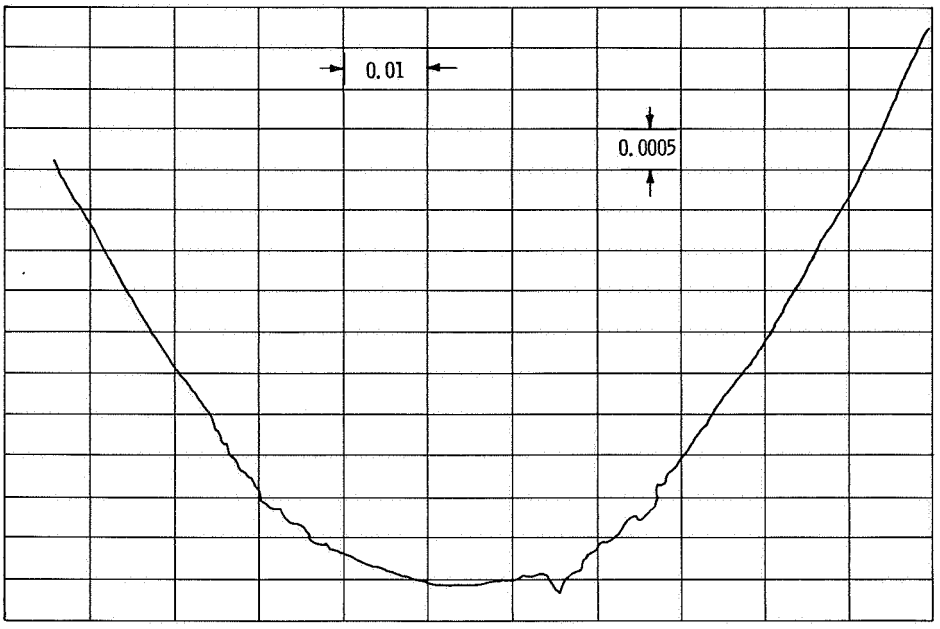

(a) Trace across damaged area of socket.

Figure 14. - Turbine journal bearing pivot surface contours.

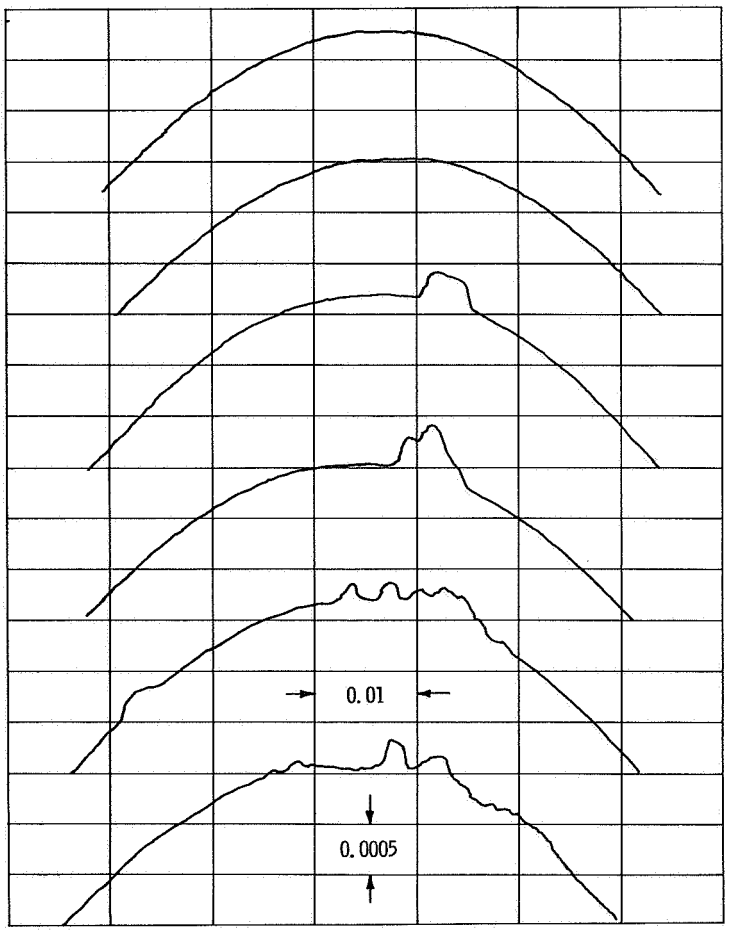

(b) Traces across damaged areas of ball.

Figure 14. - Turbine journal bearing pivot surface contours.